Review

Rising Anode-Free Lithium-Sulfur batteries

Jakob Offermann [a], Andrea Paolella [b], Rainer Adelung [a], Mozaffar Abdollahifar [a,*]

[a] Chair for Functional Nanomaterials, Department of Materials Science, Faculty of Engineering, Kiel University, Germany
[b] Dipartimento di Scienze Chimiche e Geologiche, Università degli Studi di Modena e Reggio Emilia, Via Campi 103, Modena 41125, Italy

ABSTRACT

Anode-free batteries (AFBs) represent a paradigm shift in battery architecture, eschewing conventional metal anodes in favor of current collectors (CCs). This innovative approach promises heightened energy densities, reduced manufacturing costs, and diminished environmental impact compared to traditional metal batteries. A particularly promising subset of AFBs are anode-free lithium-sulfur batteries (AFLSBs), which have garnered substantial attention due to their exceptional theoretical energy density, sulfur's abundance, and potential cost advantages. This mini-review encapsulates the recent studies in AFLSB research, elucidating key challenges and breakthroughs. The absence of a lithium (Li) metal anode mitigates safety concerns and maximizes cell energy density. However, successful Li plating on the CC necessitates a lithiophilic surface and a meticulously engineered solid electrolyte interphase (SEI). To surmount these obstacles, researchers are exploring a plethora of strategies, encompassing surface modifications, electrolyte additives, and cathode engineering. Promising results have been realized through metal coatings on CCs, utilization of 3D CCs, and incorporation of lithium polysulfide scavengers. Additionally, quasi-solid-state electrolytes offer enhanced safety and potentially augmented AFLSB performance. AFLSB research is a rapidly developing field with significant advancements being made. These breakthroughs hold the potential to usher in a new era of high-performance and sustainable energy storage solutions.

1. Introduction

The rapidly increasing global demand for high-performance energy storage systems is being driven primarily by individual mobility in the form of electric vehicles (EVs), which is expected to account for about 6000 GWh in 2030 alone.[1] In this context, the weight and volume of the battery are of crucial importance. Conventional anode/cathode materials, such as graphite[2,3] or lithium nickel manganese cobalt oxides (NMC)[4], can only store a limited amount of lithium (Li) ions in their interstitial sites [5]. In addition, as rare earth materials the components are quite expensive. Phase transformations involving an electrochemical reaction enable new storage mechanisms and allow a multiple of the previous theoretical gravimetric capacities, for example with silicon- and tin-based anodes [6]. An outstanding position in this field could be taken by sulfur (S) as a cathode storage material. Sulfur, the 16th most common element in the earth's crust, is not only abundant, but also relatively easy to extract and is low-cost. Moreover, its processing is comparatively eco-friendly [7]. With a high theoretical capacity of 1672 mAh g^{-1}, S in combination with Li is already an

intensively researched battery (Li-S battery, LSB) [3,8,9].

However, the conventional pairing of a S cathode composites with a pure Li metal anode faces essential difficulties, such as the parasitic reaction of lithium polysulfides (Li$_2$S$_x$, LiPSs) with the excessive Li metal anode (see Fig. 1). Moreover, a typically thick Li anode (several 100 μm) leads to unnecessary material costs and reduces the possible volumetric and gravimetric energy density. Decreasing the lithium thickness to a necessary minimum (< 50 μm) would improve safety and cycle stability. At the same time, the costs for the production of ultra-thin Li anodes rise disproportionately.[10] In order to circumvent these technical and economic difficulties and at the same time significantly improve the energy densities (see Fig. 1a), the interest in a completely anode-free LSB (AFLSB) based on the findings from conventional cathodes is increasing more and more in research [11,12]. Especially in the already lithiated state like Li$_2$S, but also for post-Li batteries as for example Na$_2$S (1166 mAh g^{-1}), S is an attractive electrode partner for AFLSBs, as it already has the necessary charge carriers, eliminating the need for an additional process step. Known disadvantages, such as its volume expansion of 80 %, are already present before the first cycling [13]. The

absence of the highly reactive Li metal during battery production also makes it simpler to handle the anode (e.g. Cu or Ni). Besides, Li_2S is oxygen-stable up to 220 °C and offers the potential to eliminate the need for inert atmospheres (Ar) during production. However, Li_2S is sensitive to moisture. Therefore, the amount of H_2O in the atmosphere must be restricted to a minimum (dry conditions) [14].

In the following, the fundamental principles of AFLSBs are discussed and existing concepts are highlighted. Additionally, a special focus is placed on the influence of the current collector (CC) (see Fig. 1b) and solid electrolyte interphase (SEI) modifications.

2. Fundamentals of Anode-Free Lithium-Sulfur batteries (AFLSBs)

AFLSBs are a promising battery technology that aims to improve the energy density, safety, and cost of traditional Li-S batteries. In contrast to conventional Li-S batteries that utilize a lithium metal anode, AFLSBs employ a hostless anode, typically a bare CC such as copper (Cu) foil, onto which lithium is plated during the charging process. This approach eliminates the need for excess lithium metal, reducing the weight and cost of the battery while potentially mitigating safety hazards associated with lithium metal anodes. The working principle of an AFLSB is based on a fully lithiated sulfur cathode (Li_2S) and a bare CC on the anode side (Fig. 2). The operation of AFLSBs involves the reversible lithium plating/stripping on the CC. During the initial charging step, lithium ions are extracted from the Li_2S cathode and deposited onto the CC,

forming a lithium metal anode in situ. This process is accompanied by the formation of a SEI layer on the newly formed lithium metal surface. The SEI layer is a critical component of the battery, as it helps to protect the lithium metal anode from further reactions with the electrolyte while allowing for lithium-ion transport. Upon discharge, the lithium metal is stripped from the CC and the lithium ions return to the cathode. The efficiency of lithium plating/stripping is crucial for the performance and stability of AFLSBs.[10,15–17].

AFLSBs, while sharing the fundamental concept of lithium plating onto a CC during charge, exhibit distinct reaction mechanisms compared to anode-free Li-metal batteries (AFLMBs) with conventional cathodes like Lithium Nickel Manganese Cobalt Oxide (NMC) or $LiFePO_4$ (LFP). The primary difference lies in the presence of LiPSs generated during the sulfur redox reactions. As one example: *Nanda et al.* [18] investigated the electrochemical performance of a Li-S cell utilizing a Li_2S cathode and a Cu CC. The authors highlight that the Cu $\|$ Li_2S full cell exhibited superior performance, particularly in terms of capacity retention and CE, compared to a similar cell configuration employing an LFP cathode (Cu $\|$ LFP). The authors attribute this performance enhancement to the presence of LiPSs in the AFLSB system. They explained that these LiPSs, particularly Li_2S_4, react with unevenly deposited lithium, promoting a more homogeneous lithium growth and mitigating dendrite formation. The polysulfides also contribute to a "self-healing" behavior at the interface of the deposited lithium, further enhancing the stability of the lithium deposition process [18]. This chemical interaction between LiPSs and the plated lithium is unique to Li-S batteries and is not
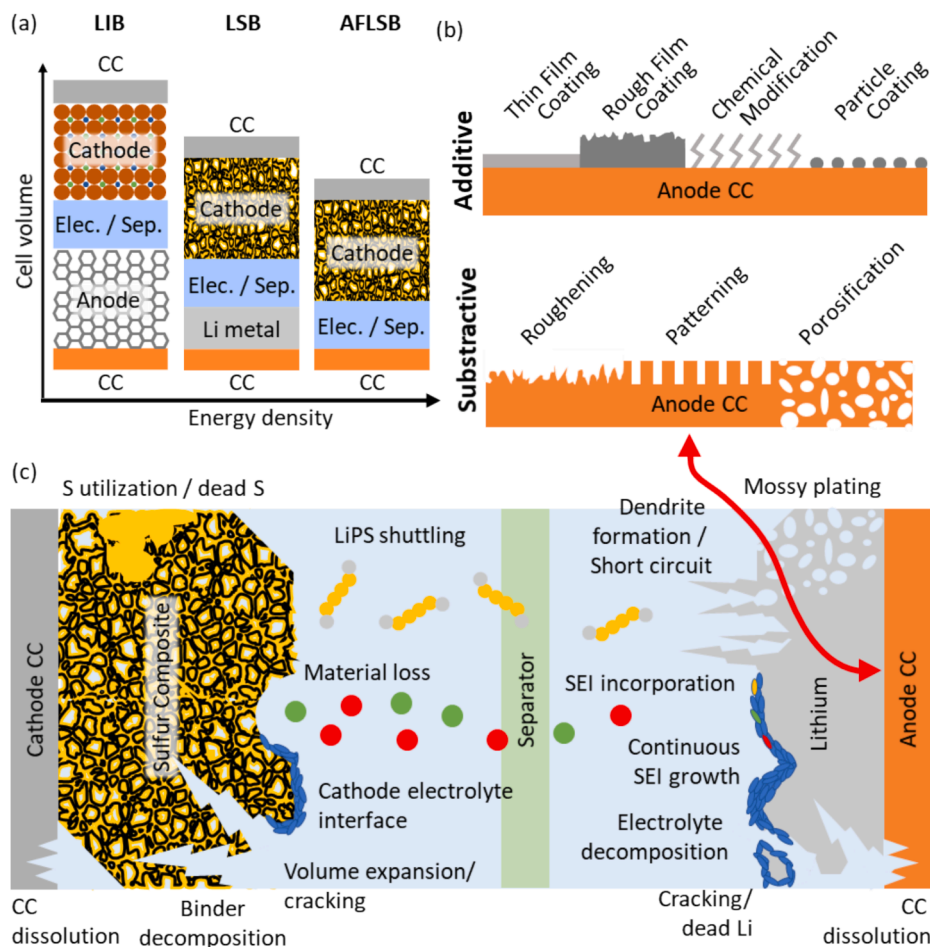

Fig. 1. (a) Advantage of anode-free lithium-sulfur batteries (AFLSBs): Cell volume vs. energy density for a typical Li-ion battery (LIB), a Li-S battery with a thick Li metal anode (LSB), and an AFLSB with their theoretic reduction in volume as a stack battery compared to LIBs. (b) Types of current collector (CC) modifications for improved Li plating and stripping in AFLSBs by additive and subtractive fabrication processes. (c) General difficulties of LSBs including cathode and anode and the incorporation of modified CC on the anode side.
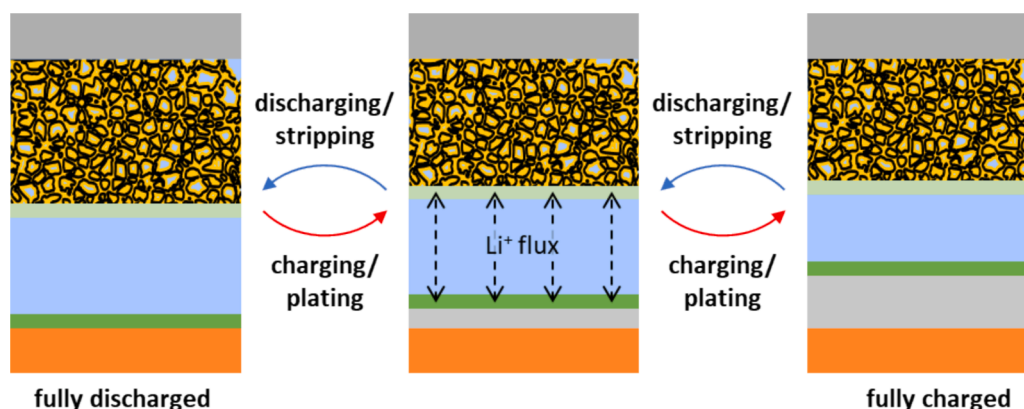
Fig. 2. Working principle of an AFLSB, starting from the initial state with a fully lithiated cathode (Li_2S) and a bare anode CC. The first charging step leads to the nucleation of Li metal on the anode CC, SEI formation and further deposition until the battery is fully charged (unlithiated S cathode, right image). The following discharge initiates Li-stripping (middle image) until the cathode is fully lithiated again. The SEI is preserved for further cycles (left image). For homogeneous Li nucleation, plating and stripping, a lithiophilic anode surface and a homogeneous Li flux, which is influenced by the SEI, are essential.

observed in AFLMBs with intercalation-based cathodes such as LFP. In a Li-S cell without polysulfides (like a control cell with just a Li metal anode and a Cu CC, or Li || Cu), lithium continues to deposit in the form hotspots, leading to the growth of dendrites – a nonuniform, high-surface-area lithium deposit [19–21]. However, this behavior could be improved by current collector and electrolyte modifications [12,22,23]. While learnings from AFLMBs with intercalation-based cathodes, such as strategies for CC modification and electrolyte engineering, can provide valuable insights, AFLSBs require careful consideration of the LiPS chemistry and its influence on the anode interface. A significant contribution to the morphology of the coating is caused by the lithiophilicity of the CC surface [24], which describes the preferential Li plating of the metal ions on the CC and is thus important for a homogeneous nucleation and subsequent dendrite-free growth. Understanding the interplay between the sulfur redox reactions at the cathode and the lithium plating/stripping processes at the anode is crucial for developing efficient and stable AFLSBs.

2.1. Advantages of AFLSBs

High energy density: The absence of excess lithium in AFLSBs allows for higher energy density compared to traditional Li-S batteries. This is because the excess lithium in traditional Li-S batteries adds weight and volume to the battery without contributing to the overall capacity. By eliminating the excess lithium, AFLSBs can achieve a higher energy density, making them more attractive for applications where weight and volume are critical factors, such as electric vehicles and portable electronic devices.

Improved safety: Eliminating the lithium metal anode reduces the risks associated with handling lithium foils and lithium reactivity. AFLSBs, by eliminating the lithium metal anode, can significantly improve battery safety.

Simplified manufacturing: The anode-free configuration simplifies the manufacturing process and reduces material costs. Traditional Li-S batteries require the use of thin lithium metal foils, which are difficult to handle and process. AFLSBs, on the other hand, can be manufactured using more readily available and easier-to-handle materials, such as Cu foils, which can simplify the manufacturing process and reduce costs.

2.2. Comparative analysis of anode-free chemistries

To better understand the potential of AFLSBs, it's crucial to compare them with other anode-free battery chemistries [12,22]. This analysis helps to identify the unique advantages and challenges associated with each technology, guiding future research directions. To calculate the

theoretical specific energy of anode-free batteries, we use the formula:

$$E_{specific} = V_{cell} \times C_{specific} \qquad (1)$$

Where: $E_{specific}$ is the theoretical specific energy (Wh kg^{-1}), V_{cell} is the average operating voltage of the battery (V), $C_{specific}$ is the specific capacity of the cathode material (mAh g^{-1}).

Table 1 presents a comprehensive overview of promising cathode materials for various anode-free battery chemistries. It details the theoretical and practical capacities of each material, along with the nominal voltage and calculated specific energy densities for pure cathodes. However, it's important to note that the actual energy density of a cell is influenced by various factors, including the electrolyte, binder, conductive carbon, current collector, cell casing, and, in the case of large batteries, modules and housing. Among the chemistries listed, AFLSBs, which utilize Li_2S as the cathode, exhibit the highest theoretical and practical specific energy values. This exceptional energy density, coupled with the abundance and cost-effectiveness of sulfur, positions AFLSBs as a compelling candidate for future energy storage solutions. However, AFLSBs also face unique challenges, primarily the polysulfide shuttle effect and lithium dendrite formation. These issues can lead to capacity fading, poor cycling stability, and safety concerns. Despite these challenges, ongoing research is actively pursuing innovative solutions to mitigate the drawbacks of AFLSBs.

Table 1

Comparison of theoretical and practical specific energies for various anode-free battery chemistries.

Anode-free Chemistry	Cathode Material	Theoretical/ Practical Capacity (mAh g^{-1})	Nominal Voltage (V)	Theoretical/ Practical Specific Energy (Wh kg^{-1})
Li-metal	LiCoO$_2$ (LCO)	~274/~140	~3.7	~1013/~518
	LiFePO$_4$ (LFP)	170/~160	~3.2	~544/~512
	LiNi$_{0.8}$Co$_{0.1}$Mn$_{0.1}$O$_2$ (NCM811)	~275/~200	~3.6	~990/~720
Na-metal	Na$_3$V$_2$(PO$_4$)$_3$ (NVP)	~117/~100	~3.4	~397/~340
	Na$_{0.7}$MnO$_2$	~240/~150	~3.2	~768/~480
K-metal	K3V2(PO4)3	~106/~85	~3.6	~381/~306
Al-metal	Graphite	~60/~50	~2.0	~120/~100
Mg-metal	Mo$_6$S$_8$	~122/~100	~1.1	~134/~110
Zn-metal	ZnMn$_2$O$_4$	~224/~175	~1.3	~291/~227
Li-S	**Li$_2$S**	**~1166/ ~850**	**~2.2**	**~2565/ ~1870**

2.3. Challenges of AFLSBs

Lithium dendrite formation: Uncontrolled lithium dendrite growth during plating can lead to short circuits and capacity fading. Even though AFLSBs eliminate the use of lithium metal anodes, lithium dendrites can still form on the CC during the lithium plating process. These dendrites can lead to short circuits and reduce the cycle life of the battery.

Polysulfide shuttle effect: The dissolution and migration of LiPSs from the cathode to the anode can result in capacity loss and poor cycling stability. These species can dissolve in the electrolyte and migrate to the anode, where they can react with the lithium metal and form insoluble sulfides, leading to capacity loss and poor cycling stability.

SEI instability: The SEI layer formed on the lithium metal anode can be unstable, due to the dynamic nature of the lithium plating and stripping process, leading to continuous electrolyte decomposition and capacity fading. This instability can lead to continuous electrolyte decomposition, which consumes active lithium and reduces the overall capacity of the battery.

As discussed in this section, the performance of AFLSBs is highly dependent on the efficient lithium plating/stripping on the CC, as well as the formation of a stable SEI layer. Additionally, the electrolyte plays a critical role in facilitating ion transport and influencing the overall battery chemistry. To achieve optimal performance and stability, researchers have focused on modifying CCs, tailoring the SEI layer composition, and developing advanced electrolyte systems. In the following sections, we will discuss recent advancements in these areas.

3. Current collector development

Manthiram's group is the pioneer for developing AFLSB, in 2018, they presented the first full cell with a bare Cu CC as an anode and a Li_2S cathode [18]. This work highlighted the beneficial effect of Li_2S_x species, so-called LiPSs, on the Li plating on a plain Cu CC. LiPSs are formed as highly reactive and mobile intermediates from S_8 to Li_2S [19]. The initial deposition of metallic lithium is heterogeneous, with field effects leading to localized hotspots of concentrated Li^+ ion flux. In the Cu || Li control cell, this leads to the growth of a high-surface area and nonuniform lithium deposit. However, in the Cu || Li_2S full cell, polysulfides, react with these inhomogeneities and form Li_2S_2 and Li_2S, neutralizing their field effects and promoting a more uniform and compact lithium deposit (Fig. 3c,d). As a result, the first unoptimized AFLSB full cell already showed an initial discharge capacity of 919 mAh g^{-1}, and a capacity retention of 51.5 % over 100 cycles and an average CE of 97.2 % over the first 50 cycles in a 1,2–dimethoxyethane (DME)/1,3–dioxolane (DOL) solution (volume ratio = 1:1) containing 2 mol L^{-1} lithium trifluoromethanesulfonate (LiCF$_3$SO$_3$) and 0.2 mol L^{-1} lithium nitrate (LiNO$_3$).

To circumvent the lithiophobic character of Cu CC, additional coatings were used next to alternative CC materials made of 100 % Ni or stainless-steel CCs. *Chen et al.* used an 80 nm thick Au foil placed on a standard Cu CC, which drastically changes the lithiophobic character to a lithiophilic surface and thus significantly reduces the nucleation barrier [25]. It is important to note that the additional coating should not increase the anode (e.g. CC) weight and cost too much, as otherwise the positive effect of the anode-free approach is reduced regarding the gravimetric capacity, and from an economic point of view, the same applies to the price. In Chen's study, the onset by the additional coating was only 0.168 mg cm^{-2} and 0.008 \$ cm^{-2}. The cell performance showed an initial discharge capacity of 770 mAh g^{-1} (20.3 % more than without additional Au coating) and further stable cycling over 150 cycles with a capacity retention of 53 % in a common electrolyte of 1 mol L^{-1} lithium bis(trifluoromethanesulfonyl)imide (LiTFSI) and 0.75 mol L^{-1} LiNO$_3$ in DOL and DME (1:1, v/v).

Other coating options include other noble metals such as silver (Ag), but also non-metals such as carbon or phosphorus, as seen in the study by *Zhao et al.* [26]. The coating of black phosphorus (BP) on Cu CC, did not only influence the lithiophilicity, but also contributed to the SEI composition. BP, for instance, reacts with the LiPSs and forms Li_7PS_6 in the SEI, which is highly ionically conductive for Li-ions and thus favors reversible Li plating/stripping.

Using a combination of 3D CCs [12] and a lithiophilic layer on CC surface, as devised by *Cheng et al.* [27], is particularly advantageous. Here, a Cu sponge mesh with a 100 nm thick Ag layer prepared by thermal evaporation was used to reduce the local current density and create space for volume expansion through the increased surface area on
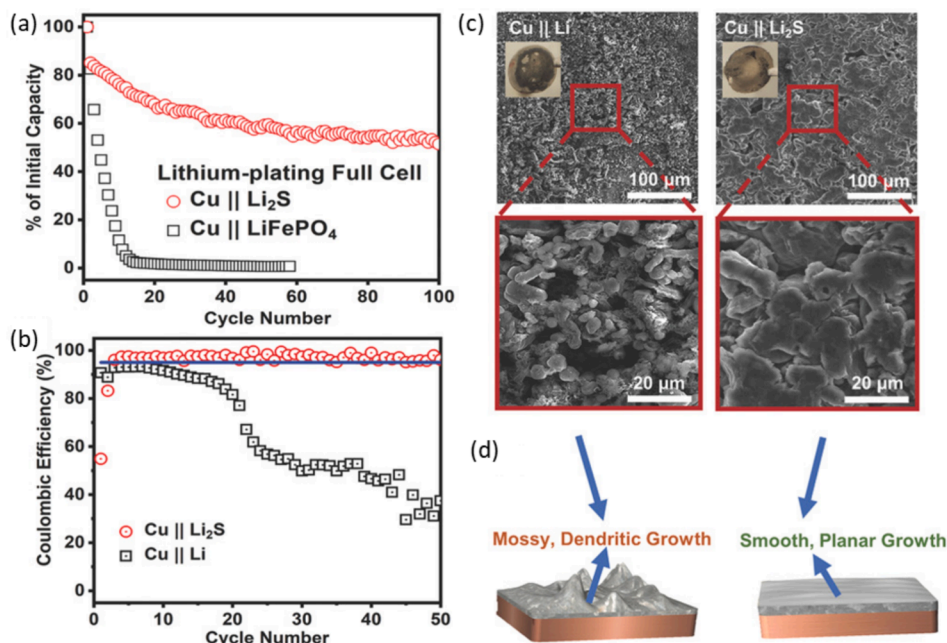

Fig. 3. Benefit of LiPSs on Li plating: a) Capacity retention of Li-plating full cells with Li_2S and LiFePO$_4$ cathodes. b) Coulombic efficiency of Cu || Li_2S full cell and Cu || Li control cell. c) SEM images and d) schematic illustration of the Li deposited in the Cu || Li control cell and Cu || Li_2S full cell, with strikingly different morphologies. Reprinted with permission [18].

the one hand and to enable a reduced nucleation barrier and smoothing of the plating layer on the other hand. In this way, an initial CE of 70.7 % was achieved with the electrolyte of 1 mol L^{-1} LiTFSI and 1 wt% LiNO$_3$ in DOL/DME (1:1, v/v), and high C-rate values were generated by the open anode system. Even ultra-high S mass loadings of 14.6 mg cm^{-2} showed an initial capacity of 7.4 mAh cm^{-2}.

A deeper understanding of the mechanisms and influencing factors is also necessary, which is investigated by *Weret et al.* [15] through in situ studies of the effect of generated LiPS redox species on the electrochemical performance of a Li$_2$S cathode and Cu CC (anode). They demonstrated during battery cycling, inactive Li within the battery is restored by PS redox species that helps to maintain the structure of plated Li during charging. This reactivation process could be a key to the long-lasting performance of AFLSBs.

To sum up, the development of CCs for AFLSBs has seen significant advancements, with a focus on enhancing lithophilicity and increasing surface area. Strategies such as metal coatings, 3D architectures, and the incorporation of lithium polysulfide scavengers have shown promising results in improving lithium plating/stripping efficiency and mitigating dendrite formation.

4. Electrolyte developments

The specific SEI formation is also of great importance as an interphase between the anode and electrolyte, because it co-regulates the Li plating/stripping, avoiding continuous degradation of liquid electrolytes. The SEI consists mainly of the electrolyte components. The salts and additives investigations are discussed as follows.

4.1. Electrolyte salts

Nanda et al. [28] investigated the influence of Li salts on the SEI composition and the battery performance within a Ni || Li$_2$S full cell (see Fig. 4a). Here, the salts were successively investigated under constant electrolyte conditions (50 vol% DOL + 50 vol% DME + 0.1 mol L^{-1} LiNO$_3$). It was found that 1 moL L^{-1} LiTFSI has a thinner and

correspondingly more ionically conductive SEI compared to 1 moL L^{-1} lithium bis-(fluorosulfonyl) imide (LiFSI), which has a single F group instead of a CF$_3$ group. This results in a more homogeneous Li$^+$ ion flux and more uniform Li plating. In contrast, the Li layer grown under LiFSI is mossy and leads to further side reactions, as the S-F bonds of the salt are easily broken in the presence of LiPS. The F-C bonds of LiTFSI, in contrast, are more stable. In order to evaluate the influence of nitrogen in the SEI, the salt lithium triflate (LiCF$_3$SO$_3$), which does not contain nitrogen, was compared with LiTFSI. Here it was shown that the formation of Li$_3$N in the SEI improves the Li-ion conductivity [29]. This was also confirmed by omitting LiNO$_3$ as an electrolyte additive (see Fig. 4b-d). Moreover, the NO$_3^-$ anions from LiNO$_3$ oxidize the reduced sulfur atoms to form Li$_2$SO$_3$ and Li$_2$SO$_4$ on the SEI surface, which passivate and stabilize it.

As an expansion to the best performing electrolyte composition (1 mol L^{-1} LiTFSI + 0.2 mol L^{-1} LiNO3 in DOL DME (1:1, v/v), *Yen et al.* [30] added neodymium trifluoromethanesulfonate, so-called neodymium triflate (Nd(OTf)$_3$), as a further electrolyte salt in order to transfer the advantages of rare earth compounds as a cathode component to the electrolyte. An optimized amount of only 1.5 mmol L^{-1} Nd(OTf)$_3$ showed an improvement of the liquid-to-liquid sulfur conversion kinetics as well as LiPS adsorption both at half-cell and full-cell level (Ni || Li$_2$S). At the same time, Nd-S is embedded within the anode SEI, which allows a more compact Li deposition by lowering the necessary overpotential. Enhanced Coulombic efficiency (CE), higher initial capacities (793 mAh g^{-1} vs. 709 mAh g^{-1} without Nd(OTf)$_3$ additive) and a longer lasting battery are the result even at an increased loading density of 5.5–7.0 mAh cm^{-2}.

4.2. Electrolyte additives

However, not only the salt alone determines the SEI composition. *Asano et al.* [31] employed highly concentrated 1.6–3 mol L^{-1} LiTFSI/ LiFSI (9:1 M ratio) in sulfolane electrolytes, which reduced the LiPS solubility and mitigated the LiPS shuttle effect. In addition, a particularly fluorine-rich SEI with more than 12.62 % was formed by the
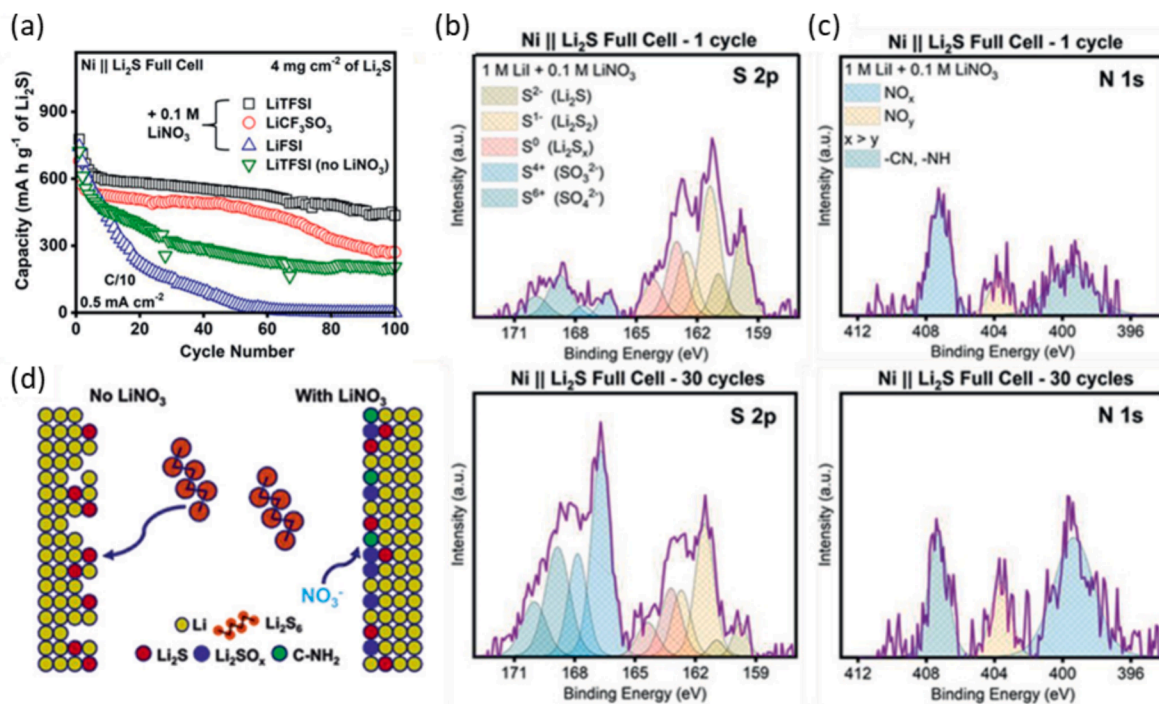

Fig. 4. A) electrochemical results of ni || li$_2$S full cells with the different electrolytes. b) S 2p spectra (XPS) for deposited Li with LiI + LiNO$_3$ with oxidized sulfur species (SO$_3^{2-}$, SO$_4^{2-}$) by LiNO$_3$. c) N 1 s spectra for the interface showing nitrite (NO$_2^-$) and organic nitrogenated species. d) Schematic illustration of the proposed mechanism underlying the role played by nitrate oxidation of sulfides into sulfates in stabilizing the surface of Li metal. Reprinted with permission [28].

decomposition of the anions (especially FSA⁻) (control sample 1 moL L⁻¹ LiTFSI/LiFSI: 2.50 %) and at the same time the O species were reduced, which led to a more homogeneous Li plating. The cyclability improved when the temperature was increased during the initial cycle up to 60 °C.

Other additives have also been tested in AFLSBs to optimize the SEI composition for improved Li plating and stripping. *Liao et al.* [32] used fumed SiO₂ nanoparticles in ether-based electrolyte with 1 moL L⁻¹ LiTFSI and 2 wt% LiNO₃. Also here, the formation of LiF within the SEI, which is favorable for Li⁺ conductivity and flux, was increased by the partial adsorption of TFSI⁻ ions by SiO₂ followed by the reduction of TFSI⁻ when the SiO₂ is co-deposited with Li⁺. In addition, the hydroxyl groups on the particle surfaces in the electrode/electrolyte interface promoted Li ion transport, enabling 523 mAh g⁻¹ with a Cu anode and Li₂S cathode after 200 cycles (initial 1055 mAh g⁻¹).

Meanwhile, *Ren et al.* [33] added 0.2 mol L⁻¹ SnI₂ and LiI to the ether electrolyte. During the initial cycle, oxidized Sn formed soluble SnI₄-LiPS complexes, which interacted with other LiPS, for example promoting further transport of LiPS within the cell or facilitating the S conversion. The complexes also led to Sn accumulation in the SEI in the form of Li₂SnS₃. The SEI addition produced a smoother and more stable Li surface after plating on a Ni anode, resulting in a capacity retention of 78.2 % after 100 cycles (0.1 C). Other 5th-period post-transition metal iodides were also investigated (In, Sb) and showed comparable results in terms of SEI composition and Li plating morphology. However, they

were disadvantageous in terms of solubility and LiPS interaction. In these studies, SnI₂ showed the best overall results.

Tellurium has been successfully tested as an effective additive at the cathode side by the Manthiram's group (see section 5 Cathode and separator optimizations) [34,35], as it reacts with the LiPSs (Li₂TeₓSᵧ) and is incorporated into the SEI, improving the diffusion of Li. A completely new form of Te incorporation with great potential is lithium tritelluride (LiTe₃) as an electrolyte additive. The LiTe₃ synthesized by *Lai et al.* [36] from the reaction of LiH and Te in DOL/DME dissolved in the electrolyte and, like elemental Te or TeNW, reacted with LiPSs to form a Li₂TeS₃ and Li₂Te-rich SEI. With a concentration of 0.1 mol L⁻¹ in the electrolyte, a full cell with Ni anode reached 350 mAh g⁻¹ after 100 cycles and thus 71 % of the initial capacity, whereas the capacity of the reference cell dropped to 23 %.

4.3. Quasi solid-state electrolytes

Quasi-solid-state electrolytes (QSE) represent a promising technology due to their high ionic conductivity and good processability [37,38]. Moreover, a solid electrolyte matrix prevents liquid electrolyte from leaking out of the battery cell increasing the level of safety with respect to LIBs. Li dendrite growth can be suppressed, which eliminates harmful short circuits. In addition, the solid electrolyte prevents the LiPS from migrating and is therefore particularly attractive for sulfur cathodes in
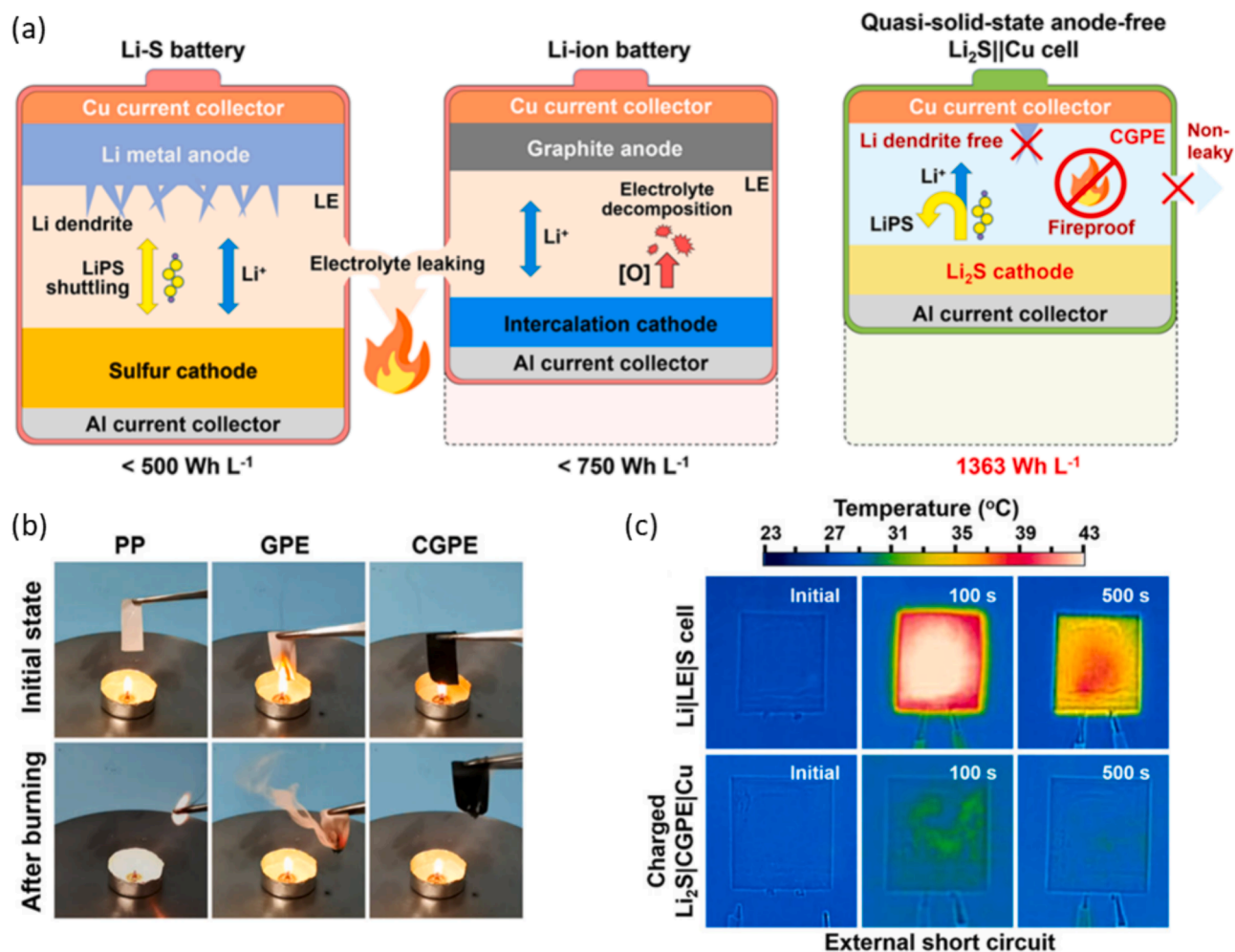

Fig. 5. A) schematic illustration of the quasi-solid-state li₂S ‖ Cu cells. Schematic configurations and advantages of quasi-solid-state Li₂S ‖ Cu cells in satisfying both high energy and reliability by stable redox chemistry in robust and fire-retardant gel polymer electrolyte. (The LE, CGEP, LiPS and [O] refer to the liquid electrolyte, composite gel polymer electrolyte, lithium polysulfides and radical oxygen, respectively.). b) Flame test of PP, MXene-free GPE and CGPE. c) Infrared thermography of lithiated Li₂S@MX | CGPE | Cu full cells and Li | LE | S cells after external short circuit. Reprinted with permission [39].

combination with AFLMBs (see Fig. 5a).

Liu et al. [39] fabricated a non-flammable polymeric gel electrolyte based on poly(vinylidene fluoride-co-hexafluoropropylene) (PVDF-HFP). In addition, LiTFSI and $Ti_3C_2T_x$ MXenes were added, lowering the glass transition temperature (T_g), a cold pressing strategy was used to activate bulk Li_2S within an MXene matrix for the cathode, and thus increasing the ionic conductivity (up to 0.81 mS cm^{-1} at 25 °C). The highly conductive MXenes also mechanically reinforce the composite gel polymer electrolyte (CGPE), which compensates for the Li volume expansion during plating on the Cu anode. With a 20–30 μm thick quasi-solid electrolyte, a Cu|CGPE|Li$_2$S@MXene cell showed a capacity retention of 80 % after 300 cycles with a relatively high loading of 5 mg cm^{-2}. MXene-based CGPEs offer a promising solution to the challenges of lithium metal batteries. The high elastic modulus of MXene enhances the mechanical robustness of the CGPE, effectively withstanding the strain from lithium dendrite growth and volume changes. Simultaneously, MXene's oxygen-containing groups adsorb LiPSs, suppressing the shuttle effect that hinders stable cycling. Furthermore, the porous structure of the CGPE, coupled with MXene's excellent ionic conductivity, ensures uniform lithium-ion flux, promoting smooth lithium plating and suppressing dendrite formation and no "dead Li" [40] was formed. As a pouch cell, an energy density of 1323 Wh L^{-1} was achieved. The authors' approach faces challenges in scalability and cost-effectiveness due to the use of MXene, a relatively expensive material. Additionally, the cold-pressing method employed for cathode fabrication might pose difficulties in the electrode morphology and porosity and large-scale production. Further research is needed to assess the long-term stability of the MXene-containing batteries.

However, the field of possible polymer-additive combinations is large and holds great potential for further research. *Zhao et al.* [41] proposed a Cu || Li$_2$S cell with a QSE obtained by the combination of thermoplastic polyurethane (TPU) and nano-fumed silica aerogels (SiO$_{2-x}$(OH)$_x$) by solution-casting method. The QSE is highly hydrophobic, preventing moisture penetration and subsequent reactions with Li metal, which can lead to dendrite formation and safety hazards. After preparation, the QSE was immersed in liquid 1 mol L^{-1} LiTFSI + DOL/DME (1:1, v/v) electrolyte for 12 h. The mechanically and thermally (up to 300 °C) stable film with an ionic conductivity of 0.85 mS cm^{-1} showed a CE of 98.6 % over 100 cycles and even after 500 cycles (0.1 C) yielded 264 mAh g^{-1} (initially 681 mAh g^{-1}) without significant dendrite formation. In this study, Li$_2$S cathodes offer a major safety advantage over conventional Li-ion cathodes. Unlike NCM, which releases oxygen radicals that can react with the electrolyte causing thermal runaway, Li$_2$S is oxygen-free, eliminating this risk. This study proves this by showing an anode-free pouch cell remaining stable even when overcharged (5.0 V), while a conventional Li-S cell experiences thermal runaway. This inherent safety makes Li$_2$S a promising cathode material for next-generation batteries.

Meng et al. [42] originally intended to form an air-stable Li$_2$S cathode, the authors coated the electrode with a dense, 15–30 μm thick layer from graphene oxide (GO) interlinked poly-1,3-dioxolane (DOL) (GPD). This protected the underlying cathode from moisture for 70 h and thus demonstrated an air-lifetime that was 2000 times longer. Moreover, in a battery, the layer can be converted in situ into a gel polymer electrolyte by adding a liquid electrolyte (1 mol L^{-1} LiTFSI in DOL/DME (1:1, v/v) with 2 wt% LiNO$_3$) and heating to 55 °C for 12 h, which in the end has a high ionic conductivity of 1.1 mS cm^{-1} and at the same time minimizes the dissolution of LiPS into the electrolyte. In combination with a Cu anode coated with Ag nanoparticles, the cell demonstrated increased cycle life with a CE of 98 % over 100 cycles and in the pouch format the cell exhibited a high energy density of 1093 Wh L^{-1}.

The use of QSEs in AFLSBs offers a promising approach to enhance safety and improve performance. QSEs can suppress dendrite growth, prevent polysulfide shuttling, and provide good interfacial contact with the electrodes. The development of QSEs with high ionic conductivity and good mechanical properties is crucial for the advancement of AFLSBs and further research is needed to assess the long-term stability and performance of the QSE and to optimize the design for mass production.

5. Cathode and separator optimizations

Due to the highly mobile cell system with diffusing LiPSs, in addition to electrolyte additives, the introduction of metal species into the cathode structure is also a way of modifying the SEI. Especially if the desired additives are not or insufficiently soluble in the electrolyte. For example, Mo and W species have already been successfully incorporated by *Nanda et al.* [43]. The additives (0.05 wt%) ammonium tetrathiomolybdate ((NH$_4$)$_2$MoS$_4$) and ammonium tetrathiotungstate ((NH$_4$)$_2$WS$_4$) were used as Mo and W sources: the tetrathiometallate anions (MoS$_4^{2-}$ and WS$_4^{2-}$) subsequently reacted in several steps with the LiPSs forming new complexes (see Fig. 6a), which were able to reduce the shuttle effect. At the same time, a Mo/W-rich SEI was formed on the Ni anode. Due to their similar electronegativities to S, Mo and W can presumably lower the electron density around S and thus increase the Li-ions diffusion. The result was a more homogeneous and smoother Li plating with less side reactions, resulting in 3-times longer cycle life (50 % of initial capacity after 164 vs. 58 cycles in the control cell).

Zhao et al. [44] instead used In$_2$Se$_3$ nanosheets and improved with only 3.8 wt% both the cathode side by an increased LiPS adsorption and at the same time accelerated conversion kinetics and the anode side by embedding In and Se in the SEI. The latter found their way to the Cu anode as soluble In^{3+} and Se^{2-} ions, where they formed a compact SEI layer mainly consisting LiInS$_2$ and LiInSe$_2$. Due to the lower diffusion barrier of LiInS$_2$, 0.286 eV, and LiInSe$_2$, 0.269 eV, compared to Li$_2$S, 0.348 eV, Li could be further plated more homogeneously. A high CE of 98.3 % over 160 cycles and a capacity of 515 mAh g^{-1} could be tested with a loading of 4 mg cm^{-2} Li$_2$S and a low electrolyte-to-solid ratio of 7.5:1 under 0.2 C.

In particular, tellurium was tested as an SEI additive at the cathode side by the Manthiram's group. *Nanda et al.* [34] embedded elemental tellurium in their Li$_2$S cathode (10 wt%). Also in this case, Te was oxidized with the LiPSs and formed soluble polytellurosulfide species (Li$_2$Te$_x$S$_y$), which could diffuse to the Ni CC side. The subsequent reduction formed an SEI of Li$_2$TeS$_3$ and Li$_2$Te, whereby two regions were identified. The main Li$_2$TeS$_3$ amount was detected in the SEI region facing the electrolyte. Due to the small electronegativity difference (S: 2.58, Te: 2.1), the Te-S bond in Li$_2$TeS$_3$ has a slight covalent character, which first reduced the electron density of the S atoms and consequently lowered the diffusion barrier of the Li ions. Li$_2$Te, which occurs throughout the SEI, can also promote the diffusion of Li due to the large size of the Te anion and its higher polarizability compared to Li$_2$S (see Fig. 6b,c). In the Ni || Li$_2$S + 0.1 Te full cell, Nanda showed a 50 % capacity loss not before 240 cycles and thus demonstrated a 7-fold longer cycle stability compared to the full cell without Te addition. Even as an LSB pouch cell (Li || S + 0.1 Te) with a low E/S ratio of 4.5 μL mg^{-1} and an S loading of 5.2 mg cm^{-2}, the addition of tellurium extended the cycle stability so that a drop in capacity retention down to 50 % of the initial capacity was able to be increased from 25 cycles to more than 100 cycles.[34].

Due to the high cost of Te further methods were explored to lower the required amount. In this context, nanowire structured Te (TeNW) was developed by *Sul et al.* [35] and used as a separator coating or directly as an anode material. The TeNWs produced by a hydrothermal production process were approx. 9 nm in diameter and consisted out of a Te core and a 10 wt% outer carbon coating, which remained as a residue of the PVP starting material. As a separator coating, only 4 wt% (0.13 mg cm^{-2}) TeNW was sufficient to effectively enhance the reaction of Te with LiPS compared to the Li$_2$S mass (see Fig. 6d). The same applies to TeNW + CNT (1:9 mass ratio) as anode material, whereby 532 mAh g^{-1} and thus 57 % of the initial capacity was achieved after 200 cycles.
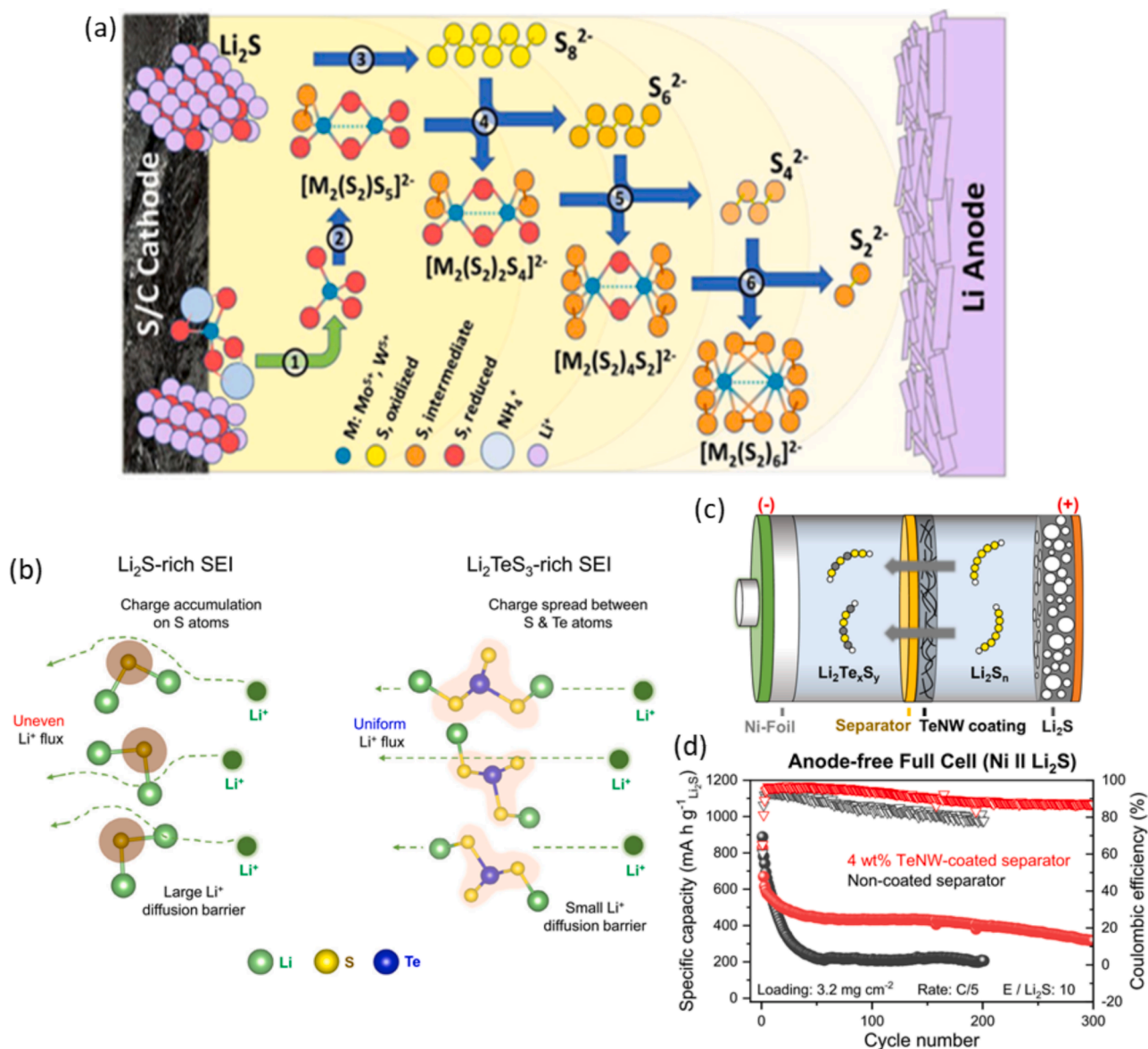
Fig. 6. (a) A schematic depiction of the introduction of the MS_4^{2-} species into the electrolyte, its dimerization, and spontaneous reaction with long-chain LiPSs through S^0 atom uptake. The acid-base step is shown with a green bent arrow, while the steps involving intra-/intermolecular redox transformations are shown with blue arrows. Reprinted with permission [43]. (b) Schematic of the Li-ion diffusion trend in conventional Li_2S-rich and Li_2TeS_3-rich SEI. (c) Schematic of AFLSB cell configuration. (d) Long-term cycling performance of 4 wt% TeNW-coated separator and uncoated separator cells. Reprinted with permission [35].

Furthermore, non-metal species can also have a positive effect on the SEI composition and the resulting Li plating. For instance, *Sul et al.* [45] demonstrated that a cathode coating with Li_2CS_3 not only holds the LiPSs physically and chemically and thus reduces the shuttle effect, but also increases the proportion of reduced S species (Li_2CS_3) in the anode SEI and simultaneously reduces the oxidized species (SO_3^{2-}/SO_4^{2-}). In this case, Li_2CS_3 acts similarly to Li_2TeS_3 and has a more covalent character compared to Li_2S, which changes the electron density between C and S and reduces the Li ion diffusion barrier. The resulting more homogeneous Li-ion flux favors Li plating and morphology and enables 51 % capacity retention (330 mAh g^{-1}) after 125 cycles. In addition, the average discharge voltage increases by 0.12 V to 2.23 V and thus improves the energy density.

It should always be kept in mind that a general improvement in the S-cathode can be expected to improve the AFLSB. One example is *Jin et al.* [46] who used a functional binder composite of poly(ethylene oxide) (PEO) with a cross-linked functionalization (MHPP) as the skeleton for the Li_2S cathode in combination with a anode-free nickel CC. The MHPP

is obtained by polymerizing maleic anhydride (MAH), hexafluorobutyl methacrylate (HFBMA), poly(ethylene glycol) methyl ether methacrylate (PEGMA) and polyethylene glycol diacrylate (PEGDA). All polymers have different kind of functional groups, for example PEO has ether oxygen groups while the final MHPP could present polar C = O groups which can immobilize LiPS, thereby reducing the shuttle effect. In addition, HFBMA has C-F groups for improved electrochemical stability. The combination of MAH and HFBMA inhibits the crystallization of PEO and improves Li ion conductivity, same as with the high mobility of PEGMA and PEGDA. Compared to a PEO-PVP system, PEO-MHPP showed a significant improvement in terms of long-term stability and battery loading in a pouch cell. The cell with PEO-MHPP binder showed a 35 % higher Li_2S utilization and a 2-fold slower fade rate per cycle, especially due to the large reduction of the LiPS shuttle caused by the large number of functional groups. However, the SEI composition was also influenced by the binder choice by reducing the ionically insulating SO_3^{2-}/SO_4^{2-} compounds and increasing the LiF concentration, which facilitated electron shielding. Also catalysts are of increasing interest in

standards LSB research.[47–49] *He et al.* [50] employed the known advantages of cobalt in the form of Co and Co_9S_8 to reduce LiPS shuttling and accelerate the conversion of S to Li_2S. For the cathode production, Li_2SO_4 and $CoSO_4$ were mixed with 80 % L_2S. During the carbothermal reduction, Co and Co_9S_8 served as nucleation sites to ensure a uniform distribution of Li_2S in the composite, which also improved the later Li_2S utilization. The addition of 8 wt% Te led to a further stable protective layer on the Li_2S-Co_9S_8/Co cathode and improves battery performance by reducing LiPS shuttling and SEI embedding (see above). A Li_2S cathode with Co_9S_8/Co and Te thus achieved a capacity of 865 mAh g^{-1} after 100 cycles (0.1C), whereby the initial CE was already 85 %.

This section highlights the critical role of cathode and separator modifications in enhancing the performance of AFLSBs. By incorporating metal or non-metal species into the cathode structure or separator, researchers can effectively modify the SEI on the lithium anode, leading to improved lithium plating, reduced polysulfide shuttling, and ultimately, enhanced cycle life and capacity retention.

6. Conclusions and perspectives

6.1. Conclusion

This mini-review has explored AFLSBs as a rising technology in the field of energy storage.

AFLSBs offers several advantages over conventional LIBs, including higher energy density, improved safety, and reduced cost. The absence of an excess lithium anode in AFLSBs allows for more active material within the same volume, leading to higher gravimetric and volumetric

Table 2
Summary of AFLSB literature with respect to the associated improvement strategy.

AFLSB strategy	Parameter	Cell Design	Electrolyte[a] (E/S ratio)	Mass Loading [mg cm^{-2}]	Cycles / C-rate Potential Window	init. Capacity [mAh g^{-1}] / init. CE	fin. Capacity [mA h g^{-1}] / ave. CE	Ref.
Current Collector	general function of Li deposition / stripping	Cu ‖ Li$_2$S	E$_{STD}$ + 2 wt% LiNO$_3$ (N/A)	2.36	200 / 0.1C 1.8–2.8 V	697 / 56.5 %	393 / 96.2 %	[15]
	80 nm Au foil	Cu + Au ‖ Li$_2$S	E$_{STD}$ + 0.75 mol L^{-1} LiNO$_3$ (12:1)	4	150 / 0.05C 1.7–2.8 V	770 / 69.5 %	408 / N/A	[25]
	bare Cu (pioneer work)	Cu ‖ Li$_2$S	2 mol L^{-1} LiCF$_3$SO$_3$ in DOL/DME + 0.2 mol L^{-1} LiNO$_3$ (20:1)	4	100 / 0.1C 1.8–2.8 V	639 / 65.8 %	329 / 96.0 %[b]	[18]
	Ag coating on 3D Cu	3D Cu + Ag ‖ Li$_2$S	E$_{STD}$ + 1 wt% LiNO$_3$ (N/A)	3.8	180 / 0.1C 1.7–2.8 V	752 / 70.7 %	424 / 97.0 %	[27]
	black phosphorus coating	Cu + BP ‖ Li$_2$S	E$_{STD}$ + 5 wt% LiNO$_3$ (5:1)	4	100 / 0.2C 1.7–2.8 V	773 / 70.7 %	501 / N/A	[26]
Electrolyte	Li salts (LiTFSI, LiFSI, LiCF$_3$SO$_3$, LiNO$_3$)	Ni ‖ Li$_2$S	different salts in DOL/DME (excess)	4	100 / 0.1C 1.8–2.8 V	775[c] / 67.3 %[c]	435[c] / N/A	[28]
	Nd(OTf)$_3$ additive	Ni ‖ Li$_2$S	E$_{STD}$ + 0.2 mol L^{-1} LiNO$_3$ + 1.5 mmol L^{-1} Nd(OTf)$_3$ (10:1)	4	100 / 0.2C 1.8–2.8 V	793 / 84.5 %	420 / 94.0 %	[30]
	highly concentrated Li salts	Cu ‖ Li$_2$S	[Li(SL)$_2$][TFSA$_{0.9}$FSA$_{0.1}$]-2HFE (N/A)	4.3	75 / 0.42C 1.1–3.3 V	760 / 62.8 %	172 / 96.7 %	[31]
	fumed SiO$_2$ additive	Cu ‖ Li$_2$S	E$_{STD}$ + 2 wt% LiNO$_3$ (N/A)	4	200 / 0.1C 1.7–2.8 V	735 / 67.0 %	370 / N/A	[32]
	SnI$_4$ additive	Ni ‖ Li$_2$S	E$_{STD}$ + 0.5 mol L^{-1} LiNO$_3$ + 0.2 mol L^{-1} SnI$_2$/LiI (7.5:1)	4	100 / 0.1C 1.8–2.8 V	1050 / 65.0 %	619 / N/A	[33]
	LiTe$_3$ additive	Ni ‖ Li$_2$S	E$_{STD}$ + 0.25 mol L^{-1} LiNO$_3$ + 0.1 mol L^{-1} LiTe$_3$ (10:1)	3.5	100 / 0.2C 1.8–2.8 V	492 / 84.0 %	350 / 97.5 %	[36]
Cathode	Thiometallate additives	Ni ‖ Li$_2$S + ATTW	E$_{STD}$ + 0.25 mol L^{-1} LiNO$_3$ (N/A)	4–5	200 / 0.2C 1.8–2.8 V	730 / 56.5 %	320 / N/A	[43]
	In$_2$Se$_3$ nanosheet additive	Cu ‖ Li$_2$S + In$_2$Se$_3$	E$_{STD}$ + 0.2 mol L^{-1} LiNO$_3$ (7.5:1)	4	160 / 0.2C 1.7–2.8 V	858 / 90.3 %	514 / 98.3 %	[44]
	Te additive	Ni ‖ Li$_2$S + 0.1 Te	E$_{STD}$ + 0.1 mol L^{-1} LiNO$_3$ (excess)	4	240 / 0.2C 1.8–2.8 V	620 / 70.0 %	310 / 96.4 %	[34]
	Li$_2$CS$_3$ coating	Ni ‖ Li$_2$CS$_3$ @ Li$_2$S	E$_{STD}$ + 0.2 mol L^{-1} LiNO$_3$ (25:1)	3	125 / 0.2C 1.8–3.0 V	647 / 64.5 %	330 / 95.4 %	[45]
	functional binder composite	Ni ‖ Li$_2$S + PEO/MHPP	E$_{STD}$ + 0.3 mol L^{-1} LiNO$_3$ (10:1)	3.3	100 / 0.2C 1.7–2.8 V	680 / 88.0 %	355 / N/A	[46]
	Co$_9$S$_8$/Co catalyst	Ni ‖ Li$_2$S + Co$_9$S$_8$/Co + Te	E$_{STD}$ + 0.2 mol L^{-1} LiNO$_3$ (10:1)	4	100 / 0.1C 1.8–2.8 V	1025 / 85.0 %	865 / N/A	[50]
Separator	TeNW coating	Ni ‖ TeNW ‖ Li$_2$S	E$_{STD}$ + 0.25 mol L^{-1} LiNO$_3$ (10:1)	3.2	300 / 0.2C 1.8–3.0 V	831 / 65.0 %	316 / 91.3 %	[35]
Anode	TeNW @ CNT anode	Li-TeNW@ CNT ‖ S	E$_{STD}$ + 0.25 mol L^{-1} LiNO$_3$ (10:1)	2.23	200 / 0.2C 1.8–3.0 V	649 / 67.0 %	370 / 91.7 %	[35]
Quasi Solid Electrolyte	composite gel polymer electrolyte (PVDF-HFP + MXene)	Cu ‖ CGPE ‖ Li$_2$S @MXene	LiTFSI in DOL/DME (1.5:1)	5	300 / 0.2C 1.7–2.8 V	819 / 80.0 %	655 / N/A	[39]
	TPU/SiO$_{2-x}$(OH)$_x$	Cu ‖ QSE ‖ Li$_2$S	E$_{STD}$ (immersed)	2	500 / 0.1C 1.7–2.7 V	686 / N/A	264 / 98.6 %[b]	[41]
	GO + PD	Cu + Ag ‖ GPE ‖ Li$_2$S	E$_{STD}$ + 2 wt% LiNO$_3$ (N/A)	4	100 / 0.2C 1.7–2.8 V	666 / 82.0 %	399 / 98.0 %	[42]

[a] E$_{STD}$: 1 mol L^{-1} LiTFSI in DOL/DME (1:1, v/v), [b] based on first 100 cycles, [c] with E$_{STD}$ + 0.1 mol L^{-1} LiNO$_3$.

energy densities. This is particularly beneficial for applications where weight and volume are critical factors, such as electric vehicles and portable electronics. Additionally, eliminating the lithium metal anode mitigates safety hazards associated with dendrite formation and lithium reactivity, making AFLSBs inherently safer. Furthermore, AFLSBs have the potential to be more cost-effective due to the removal of lithium metal processing and the utilization of abundant and low-cost sulfur. Some other key findings are listed below:

- *Platting mechanism*: Lithium plating starts unevenly, forming "hotspots" where lithium ions concentrate. Without polysulfides (e.g., Li || Cu), these hotspots grow into dendrites, a harmful type of lithium deposit. However, polysulfides in a Li_2S || Cu cell react with these hotspots, leads to a denser, more stable structure. Polysulfides also create a dynamic interface with the lithium, constantly reacting and changing. This "self-healing" behavior counteracts uneven deposition and limits the formation of unwanted SEI components that can degrade the battery, resulting in a more stable and efficient lithium metal anode.
- The performance of AFLSBs is highly dependent on the efficient lithium plating and stripping on the CC. Recent research has focused on modifying the CC to enhance its lithiophilicity and surface area, thereby promoting uniform lithium deposition and mitigating dendrite formation.
- The composition of the SEI layer is crucial for regulating lithium plating/stripping behavior and preventing dendrite growth. Electrolyte engineering, including the use of specific additives and formation protocols, can tailor the SEI composition to improve its stability and ionic conductivity.
- QSEs offer a promising approach to enhance the safety and performance of AFLSBs by suppressing dendrite growth, prevent LiPS shuttling, and provide good interfacial contact with the electrodes, leading to improved cycling stability and overall battery performance.

Table 2 summarizes the recent advancements in AFLSBs with a focus on the strategies employed to enhance these batteries. These strategies encompass various approaches, including modifications to the current collector, electrolyte, cathode, separator, and the utilization of quasi-solid electrolytes reported in different studies. However, several challenges, such as lithium dendrite formation, polysulfide shuttle effect, and SEI instability, need to be addressed before AFLSBs can achieve widespread practical application, which will be discussed further in the subsequent section.

6.2. Key challenges

Current collector optimization:

- The success of AFLSBs critically depends on achieving uniform and dendrite-free lithium plating on the CC. This requires careful optimization of the CC's lithiophilicity and surface properties to promote uniform nucleation and growth of lithium.
- Recent research has demonstrated the effectiveness of various strategies, such as coating CCs with lithiophilic materials like noble metals (e.g., silver) or non-metals (e.g., carbon, phosphorus) to improve lithium plating behavior.
- Utilizing 3D CCs with high surface area and lithiophilic coatings further enhances lithium plating uniformity and accommodates volume changes during cycling. These 3D structures provide more sites for lithium nucleation and reduce local current density, leading to more even lithium deposition.

SEI and electrolyte optimization:

- The SEI plays a crucial role in regulating lithium plating/stripping behavior and preventing dendrite growth. A stable and ionically conductive SEI is crucial for efficient and long-lasting AFLSB performance.
- Tailoring the SEI composition through electrolyte engineering, including the use of specific additives and formation protocols, is essential for stable and long-lasting AFLSB performance. Additives can influence the SEI's chemical composition and morphology, improving its stability and ionic conductivity.
- Cathode modifications can also influence SEI formation, as demonstrated by the use of cathode additives to promote the formation of a stable inorganic–organic hybrid SEI. These additives can migrate to the anode side and participate in SEI formation, enhancing its properties.
- Solid-state electrolytes (SSEs) offer enhanced safety and potentially improved performance by suppressing dendrite growth. Ongoing research focuses on developing SSEs with high ionic conductivity and mechanical stability suitable for AFLSBs. SSEs can physically block dendrite penetration and provide a more stable interface with the lithium metal.

Cathode engineering and LiPS management:

- The absence of highly reactive Li metal in anode-free cells simplifies the handling of the anode material (e.g., Cu or Ni). Additionally, Li_2S is oxygen-stable up to 220 °C, offering the potential to eliminate the need for inert atmospheres during production. However, Li_2S remains sensitive to moisture, requiring careful control of atmospheric humidity to minimize exposure.
- Efficiently managing LiPSs generated during cycling is critical to prevent the polysulfide shuttle effect and capacity fading. LiPSs can dissolve in the electrolyte and migrate to the anode, leading to self-discharge and loss of active material.
- Advanced cathode architectures, such as hierarchical structures, functional binders, and conductive scaffolds, are crucial to mitigate these challenges and improve the overall performance of AFLSBs.
- Hierarchical structures provide multiscale porosity to accommodate sulfur expansion, enhance electrolyte infiltration, and improve electron/ion transport.
- Functional binders with strong polysulfide adsorption and high ionic conductivity can mitigate polysulfide shuttling and improve cathode stability.
- Conductive scaffolds, such as carbon nanotubes or graphene, can encapsulate sulfur and enhance the overall electrical conductivity of the cathode.
- In situ studies have highlighted the role of LiPS redox species in maintaining the structural integrity of plated lithium, suggesting their importance for long-term AFLSB performance.

To illustrate the diverse approaches employed to address the challenges in AFLSB development, Table 3 provides a comprehensive overview of various strategies and their impact on battery performance, highlighting the interplay between different battery components, including the CC, electrolyte, cathode, separator, and quasi-solid-state electrolytes, and the specific solutions implemented to enhance their functionality.

6.3. Future directions

To further advance AFLSB technology and overcome the remaining challenges, several promising research directions should be pursued:

- *Artificial SEI layers:* Develop strategies to form robust artificial SEI layers on the CC prior to cell assembly. This can enhance Li plating/stripping efficiency and prevent dendrite formation by providing a pre-formed, stable interface.

Table 3
Summary of strategies for enhancing AFLSB performance *.

Challenge	Solution Approach	Specific Solution	How it helps
Uneven lithium plating (dendrite formation)	Improve current collector	• Coating Cu with nanoparticles, carbons, etc. ‐ Using 3D Cu structures	• Enhance lithiophilicity and promote even deposition ‐ Increase surface area for more uniform lithium nucleation ‐ Improve lithium-ion conductivity for smoother plating
	Modify electrolyte	• Use highly concentrated LiTFSI/LiFSI salt mixtures ‐ Use additives to the electrolyte	• Guide lithium-ion transport for uniform deposition ‐ Control lithium deposition and SEI formation
	Use quasi-solid-state electrolytes	• Employ composite gel polymer electrolyte	• Suppress dendrite growth due to higher mechanical strength
Lithium polysulfide (LiPS) shuttle effect	Modify electrolyte	• Use additives to the electrolyte	• Trap polysulfides and prevent their migration ‐ Change polysulfide chemistry and improve SEI stability
	Modify cathode	• Use additives to the cathode ‐ Coating the cathode particles/electrodes ‐ Optimize the binder composite in the cathode ‐ Integrating catalysts to the cathode	• Trap polysulfides and prevent their migration and lithium plating, enhance reaction kinetics, and improve SEI formation ‐ React with polysulfides and improve SEI formation ‐ Enhance reaction kinetics and reduce polysulfide movement
	Modify separator	• Coating the separator	• Trap polysulfides and prevent their migration
	Use quasi-solid-state electrolytes	• Employ gel polymer electrolyte based on GO + PD	• Restrict polysulfide movement due to the gel structure
Unstable SEI layer	Modify electrolyte	• Use additives to the electrolyte	• Create a more stable SEI layer
	Modify anode current collector	• Physical and chemical functionalization ‐ Using carbon coating	• Improve SEI formation and stability. ‐ Enhance lithiophilicity
	Modify cathode	• Use additives to the cathode ‐ Optimize the binder composite in the cathode	• Improve SEI formation and stability

*The information presented here is based on the reviewed literature in this paper. It's important to note that specific performance metrics and the relative (dis)advantages of each strategy can vary depending on the specific materials/electrodes/cells used and the details of their implementation.

- *In-situ SEI modification:* Investigate methods to modify the SEI in-situ during cell operation to adapt to dynamic changes and maintain its stability. This could involve the use of redox-active additives or self-healing polymers that can repair damage to the SEI during cycling.

- *Electrolyte Additives:* Explore novel electrolyte additives that promote the formation of a stable and ionically conductive SEI. These additives can influence the SEI's chemical composition and morphology, improving its stability and ionic conductivity.
- *Solid-state electrolytes (SSEs):* Develop SSEs with high ionic conductivity, good mechanical properties, and excellent interfacial compatibility with both the cathode and the anode (CC). SSEs can physically block dendrite penetration and provide a more stable interface with the lithium metal.
- *Multifunctional electrolytes:* Design electrolytes with multiple functionalities, such as polysulfide adsorption, SEI stabilization, and dendrite suppression. This can address multiple challenges simultaneously and simplify the electrolyte formulation.
- *3D CCs:* Utilize 3D CCs with high surface area to reduce local current density and promote uniform Li deposition. These structures provide more sites for lithium nucleation and reduce local current density, leading to more even lithium deposition.
- *Lithiophilic coatings:* Develop cost-effective methods to apply lithiophilic coatings on CCs to enhance Li nucleation and suppress dendrite growth. These coatings can promote uniform lithium deposition and prevent dendrite formation.
- *Influence of pressure:* Applying pressure in AFLSBs can enhance contact, mitigating dendrite growth and promoting uniform SEI formation. While research on pressure's effect in AFLSBs is emerging, it shows promise in addressing the polysulfide shuttle effect and volume changes in the sulfur cathode. Systematic investigation is crucial to understand how pressure optimizes these batteries.
- *Effect of temperature:* Elevated temperatures can influence on the performance of AFLSBs by changing Li-ion conductivity and reaction kinetics. However, careful consideration must be given to the thermal stability of the electrolyte and the potential for increased side reactions at higher temperatures.
- *Operando techniques:* Employ operando characterization techniques, such as X-ray diffraction and microscopy, to gain real-time insights into the Li plating/stripping process, SEI evolution, and cathode degradation mechanisms. This can provide valuable information for understanding the dynamic processes occurring within AFLSBs and guide further optimization.
- *Computational modeling:* Computational modeling offers powerful tools to study anode-free batteries [12,22]. Density functional theory (DFT) can investigate reaction mechanisms and screen materials, while molecular dynamics (MD) can simulate lithium diffusion and polysulfide shuttling. Ab initio molecular dynamics (AIMD) provides insights into dynamic processes like SEI layer formation, and phase-field modeling helps understand dendrite growth and lithium platting on anode side and cathode evolution. Finally, Finite element analysis (FEA) can be employed to study mechanical stress and thermal effects, ensuring battery safety and longevity. Combining these techniques provides a comprehensive understanding of these complex systems, driving the development of better AFLSBs.

By pursuing these research directions, AFLSBs can overcome their current limitations and achieve their full potential as a high-energy, safe, and cost-effective energy storage technology.

CRediT authorship contribution statement

Jakob Offermann: Writing – original draft, Methodology, Investigation, Formal analysis. **Andrea Paolella:** Writing – review & editing, Investigation. **Rainer Adelung:** Writing – review & editing, Resources, Project administration. **Mozaffar Abdollahifar:** Writing – review & editing, Writing – original draft, Visualization, Validation, Supervision, Methodology, Investigation, Conceptualization.

Declaration of competing interest

The authors declare that they have no known competing financial interests or personal relationships that could have appeared to influence the work reported in this paper.

Acknowledgments

Data availability

No data was used for the research described in the article.

References

[1] S. Orangi, N. Manjong, D.P. Clos, L. Usai, O.S. Burheim, A.H. Strømman, Historical and prospective lithium-ion battery cost trajectories from a bottom-up production modeling perspective, J. Energy Storage. 76 (2024) 109800, https://doi.org/10.1016/J.EST.2023.109800.

[2] M. Abdollahifar, S. Doose, H. Cavers, A. Kwade, Graphite Recycling from End-of-Life Lithium-Ion Batteries: Processes and Applications, Adv. Mater. Technol. 8 (2023) 2200368, https://doi.org/10.1002/ADMT.202200368.

[3] M. Abdollahifar, P. Molaiyan, U. Lassi, N.L. Wu, A. Kwade, Multifunctional behaviour of graphite in lithium–sulfur batteries, Renew. Sustain. Energy Rev. 169 (2022) 112948, https://doi.org/10.1016/j.rser.2022.112948.

[4] H. Cavers, P. Molaiyan, M. Abdollahifar, U. Lassi, A. Kwade, Perspectives on Improving the Safety and Sustainability of High Voltage Lithium-Ion Batteries Through the Electrolyte and Separator Region, Adv. Energy Mater. 12 (2022), https://doi.org/10.1002/aenm.202200147.

[5] B.L.D. Rinkel, J.P. Vivek, N. Garcia-Araez, C.P. Grey, Two electrolyte decomposition pathways at nickel-rich cathode surfaces in lithium-ion batteries, Energy Environ. Sci. 15 (2022) 3416–3438, https://doi.org/10.1039/D1EE04053G.

[6] N. Nitta, G. Yushin, N. Nitta, G. Yushin, High-Capacity Anode Materials for Lithium-Ion Batteries: Choice of Elements and Structures for Active Particles, Part. Part. Syst. Charact. 31 (2014) 317–336, https://doi.org/10.1002/PPSC.201300231.

[7] W. Xue, L. Miao, L. Qie, C. Wang, S. Li, J. Wang, J. Li, Gravimetric and volumetric energy densities of lithium-sulfur batteries comes from a themed issue on Batteries and superca-pacitors, Curr. Opin. Electrochem. 6 (2017) 92–99, https://doi.org/10.1016/j.coelec.2017.10.007.

[8] J. Offermann, E. Gayretli, C. Schmidt, J. Carstensen, H.G. Bremes, A. Würsig, S. Hansen, M. Abdollahifar, R. Adelung, Enabling High-Performance Battery Electrodes by Surface-Structuring of Current Collectors and Crack Formation in Electrodes: A Proof-of-Concept, J. Colloid Interface Sci. 664 (2024) 444–453, https://doi.org/10.1016/J.JCIS.2024.03.065.

[9] M. Horst, J.K. Burmeister, M. Abdollahifar, S. Pillitteri, A. Kwade, A binder-free dry coating process for high sulfur loading cathodes of Li–S batteries: A proof-of-concept, J. Power Sources. 587 (2023) 233675, https://doi.org/10.1016/J.JPOWSOUR.2023.233675.

[10] Z. Xie, Z. Wu, X. An, X. Yue, J. Wang, A. Abudula, G. Guan, Anode-free rechargeable lithium metal batteries: Progress and prospects, Energy Storage Mater. 32 (2020) 386–401, https://doi.org/10.1016/j.ensm.2020.07.004.

[11] S. Liu, K. Jiao, J. Yan, Prospective strategies for extending long-term cycling performance of anode-free lithium metal batteries, Energy Storage Mater. 54 (2023) 689–712, https://doi.org/10.1016/J.ENSM.2022.11.021.

[12] P. Molaiyan, M. Abdollahifar, B. Boz, A. Beutl, M. Krammer, N. Zhang, A. Tron, M. Romio, M. Ricci, R. Adelung, A. Kwade, U. Lassi, A. Paolella, Optimizing Current Collector Interfaces for Efficient "Anode-Free" Lithium Metal Batteries, Adv. Funct. Mater. 34 (2024) 2311301, https://doi.org/10.1002/adfm.202311301.

[13] M. Shaibani, M.S. Mirshekarloo, R. Singh, C.D. Easton, M.C. Dilusha Cooray, N. Eshraghi, T. Abendroth, S. Dörfler, H. Althues, S. Kaskel, A.F. Hollenkamp, M. R. Hill, M. Majumder, Expansion-tolerant architectures for stable cycling of ultrahigh-loading sulfur cathodes in lithium-sulfur batteries, Sci. Adv. 6 (2020) eaay2757, https://doi.org/10.1126/sciadv.aay2757.

[14] S. Yang, X. Hu, S. Xu, A. Han, X. Zhang, N. Zhang, X. Chen, R.Z. Tian, D. Song, Y. Yang, Synthesis of Deliquescent Lithium Sulfide in Air, ACS Appl. Mater. Interfaces. 15 (2023) 40633–40647, https://doi.org/10.1021/acsami.3c08506.

[15] M.A. Weret, S.K. Jiang, K.N. Shitaw, C.Y. Chang, T.M. Tekaligne, J.C. Chiou, S. C. Yang, N.T. Temesgen, Y. Nikodimos, S.H. Wu, C.C. Wang, W.N. Su, B.J. Hwang, Reviving Inactive Lithium and Stabilizing Lithium Deposition for Improving the Performance of Anode-Free Lithium-Sulfur Batteries, ACS Energy Lett. 8 (2023) 2817–2823, https://doi.org/10.1021/acsenergylett.3c00622.

[16] A. Shao, X. Tang, M. Zhang, M. Bai, Y. Ma, Challenges, Strategies, and Prospects of the Anode-Free Lithium Metal Batteries, Adv. Energy Sustain. Res. 3 (2022) 2100197, https://doi.org/10.1002/aesr.202100197.

[17] Y. Tian, Y. An, C. Wei, H. Jiang, S. Xiong, J. Feng, Y. Qian, Recently advances and perspectives of anode-free rechargeable batteries, Nano Energy. 78 (2020) 105344, https://doi.org/10.1016/j.nanoen.2020.105344.

[18] S. Nanda, A. Gupta, A. Manthiram, A Lithium–Sulfur Cell Based on Reversible Lithium Deposition from a Li2S Cathode Host onto a Hostless-Anode Substrate, Adv. Energy Mater. 8 (2018) 1801556, https://doi.org/10.1002/AENM.201801556.

[19] X.-B. Cheng, J.-Q. Huang, Q. Zhang, Review—Li Metal Anode in Working Lithium-Sulfur Batteries, J. Electrochem. Soc. 165 (2018) A6058–A6072, https://doi.org/10.1149/2.0111801jes.

[20] Y. Liu, X. Meng, Y. Shi, J. Qiu, Z. Wang, Long-Life Quasi-Solid-State Anode-Free Batteries Enabled by Li Compensation Coupled Interface Engineering, Adv. Mater. 35 (2023) 2305386, https://doi.org/10.1002/ADMA.202305386.

[21] Z.W. Seh, Y. Sun, Q. Zhang, Y. Cui, Designing high-energy lithium-sulfur batteries, Chem. Soc. Rev. 45 (2016) 5605–5634, https://doi.org/10.1039/c5cs00410a.

[22] D. Petersen, M. Gronenberg, G. Lener, E.P.M. Leiva, G.L. Luque, S. Rostami, A. Paolella, B.J. Hwang, R. Adelung, M. Abdollahifar, Anode-free post-Li metal batteries, Mater. Horizons. (2024), https://doi.org/10.1039/D4MH00529E.

[23] J. Zhou, J. Qin, H. Zhan, Copper Current Collector: The Cornerstones of Practical Lithium Metal and Anode–Free Batteries, ChemPhysChem. 25 (2024) e202400007.

[24] S. Nanda, A. Gupta, A. Manthiram, Anode-Free Full Cells: A Pathway to High-Energy Density Lithium-Metal Batteries, Adv. Energy Mater. 11 (2021) 2000804, https://doi.org/10.1002/AENM.202000804.

[25] J. Chen, J. Xiang, X. Chen, L. Yuan, Z. Li, Y. Huang, Li2S-based anode-free full batteries with modified Cu current collector, Energy Storage Mater. 30 (2020) 179–186, https://doi.org/10.1016/j.ensm.2020.05.009.

[26] Y. Zhao, H. Ye, H. Zhang, D. Zhao, L. Huang, J.Y. Lee, The beneficial effects of black phosphorous modification of the anode current collector in Li-metal free Li2S-based batteries, Mater. Today Energy. 30 (2022) 101179, https://doi.org/10.1016/J.MTENER.2022.101179.

[27] H. Cheng, C. Gao, N. Cai, M. Wang, Ag coated 3D-Cu foam as a lithiophilic current collector for enabling Li 2 S-based anode-free batteries, Chem. Commun. 57 (2021) 3708–3711, https://doi.org/10.1039/D1CC00006C.

[28] S. Nanda, A. Manthiram, Delineating the Lithium–Electrolyte Interfacial Chemistry and the Dynamics of Lithium Deposition in Lithium–Sulfur Batteries, Adv. Energy Mater. 11 (2021) 2003293, https://doi.org/10.1002/aenm.202003293.

[29] U. v. Alpen, Li3N: A promising Li ionic conductor, J. Solid State Chem. 29 (1979) 379–392. https://doi.org/10.1016/0022-4596(79)90195-6.

[30] Y.J. Yen, A. Manthiram, Anode-Free Lithium-Sulfur Batteries with a Rare-Earth Triflate as a Dual-Function Electrolyte Additive, ACS Appl. Mater. Interfaces. 16 (2024) 34997–35005, https://doi.org/10.1021/acsami.4c05414.

[31] H. Asano, J. Liu, K. Ueno, K. Dokko, T. Kojima, N. Takeichi, T. Miyuki, Y. Yamakawa, M. Watanabe, Enhancing the reversibility of Li deposition/dissolution in sulfur batteries using high-concentration electrolytes to develop anode-less batteries with lithium sulfide cathode, J. Power Sources. 554 (2023) 232323, https://doi.org/10.1016/j.jpowsour.2022.232323.

[32] Y. Liao, L. Yuan, X. Liu, J. Meng, W. Zhang, Z. Li, Y. Huang, Low-cost fumed silicon dioxide uniform Li+ flux for lean-electrolyte and anode-free Li/S battery, Energy Storage Mater. 48 (2022) 366–374, https://doi.org/10.1016/j.ensm.2022.03.035.

[33] Y. Ren, A. Bhargav, W. Shin, H. Sul, A. Manthiram, Anode-Free Lithium–Sulfur Cells Enabled by Rationally Tuning Lithium Polysulfide Molecules, Angew. Chemie Int. Ed. 61 (2022) 2207907, https://doi.org/10.1002/anie.202207907.

[34] S. Nanda, A. Bhargav, A. Manthiram, Anode-free, Lean-Electrolyte Lithium-Sulfur Batteries Enabled by Tellurium-Stabilized Lithium Deposition, Joule. 4 (2020) 1121–1135, https://doi.org/10.1016/j.joule.2020.03.020.

[35] H. Sul, J. He, A. Manthiram, Tellurium Nanowires for Lithium-Metal Anode Stabilization in High-Performance Anode-Free Li–S Batteries, Small Sci. 3 (2023) 2300088, https://doi.org/10.1002/smsc.202300088.

[36] T. Lai, A. Bhargav, A. Manthiram, Lithium Tritelluride as an Electrolyte Additive for Stabilizing Lithium Deposition and Enhancing Sulfur Utilization in Anode-Free Lithium–Sulfur Batteries, Adv. Funct. Mater. 33 (2023) 2304568, https://doi.org/10.1002/adfm.202304568.

[37] É.A. Santos, L.M.S. Barros, A.F. Anna, I. Galantini, J.M. Gonçalves, R. Maciel Filho, H. Zanin, Trends in ionic liquids and quasi-solid-state electrolytes for Li-S batteries: A review on recent progress and future perspectives, Chem. Eng. J. 493 (2024) 152429, https://doi.org/10.1016/J.CEJ.2024.152429.

[38] X. Judez, M. Martinez-Ibañez, A. Santiago, M. Armand, H. Zhang, C. Li, Quasi-solid-state electrolytes for lithium sulfur batteries: Advances and perspectives, J. Power Sources. 438 (2019), https://doi.org/10.1016/j.jpowsour.2019.226985.

[39] Y. Liu, X. Meng, Z. Wang, J. Qiu, Development of quasi-solid-state anode-free high-energy lithium sulfide-based batteries, Nat. Commun. 13 (2022) 4415, https://doi.org/10.1038/s41467-022-32031-7.

[40] M. Abdollahifar, A. Paolella, "Dead Lithium" Formation and Mitigation Strategies in Anode-Free Li-Metal Batteries, Batter. Supercaps. (2024) e202400505. https://doi.org/10.1002/batt.202400505.

[41] C. Zhao, Y. Pan, R. Li, A. Hu, B. Zhou, M. He, J. Chen, Z. Yan, Y. Fan, N. Chen, M. Liu, J. Long, A safe anode-free lithium metal pouch cell enabled by integrating

stable quasi-solid electrolytes with oxygen-free cathodes, Chem. Eng. J. 463 (2023) 142386, https://doi.org/10.1016/j.cej.2023.142386.

[42] X. Meng, Y. Liu, L. Yu, J. Qiu, Z. Wang, Air-Stable Li2S Cathode for Quasi-Solid-State Anode-Free Batteries with High Volumetric Energy, Adv. Funct. Mater. 33 (2023) 1–8, https://doi.org/10.1002/adfm.202211062.

[43] S. Nanda, H.Y. Asl, A. Bhargav, A. Manthiram, Thiometallate-mediated polysulfide chemistry and lithium stabilization for stable anode-free lithium-sulfur batteries, Cell Reports Phys. Sci. 3 (2022) 100808, https://doi.org/10.1016/j.xcrp.2022.100808.

[44] Y. Zhao, L. Huang, D. Zhao, J. Yang Lee, Fast Polysulfide Conversion Catalysis and Reversible Anode Operation by A Single Cathode Modifier in Li-Metal Anode-Free Lithium-Sulfur Batteries, Angew. Chemie Int. Ed. 62 (2023) 2308976. https://doi.org/10.1002/anie.202308976.

[45] H. Sul, A. Bhargav, A. Manthiram, Lithium Trithiocarbonate as a Dual-Function Electrode Material for High-Performance Lithium–Sulfur Batteries, Adv. Energy Mater. 12 (2022) 2200680, https://doi.org/10.1002/aenm.202200680.

[46] B. Jin, T. Lai, A. Manthiram, High-Mass-Loading Anode-Free Lithium–Sulfur Batteries Enabled by a Binary Binder with Fast Lithium-Ion Transport, ACS Energy Lett. 8 (2023) 3767–3774, https://doi.org/10.1021/acsenergylett.3c01395.

[47] P. Wang, B. Xi, M. Huang, W. Chen, J. Feng, S. Xiong, Emerging Catalysts to Promote Kinetics of Lithium–Sulfur Batteries, Adv. Energy Mater. 11 (2021) 2002893, https://doi.org/10.1002/aenm.202002893.

[48] H. Chen, Z. Wu, M. Zheng, T. Liu, C. Yan, J. Lu, S. Zhang, Catalytic materials for lithium-sulfur batteries: mechanisms, design strategies and future perspective, Mater. Today. 52 (2022) 364–388, https://doi.org/10.1016/j.mattod.2021.10.026.

[49] F. Shi, L. Zhai, Q. Liu, J. Yu, S.P. Lau, B.Y. Xia, Z.L. Xu, Emerging catalytic materials for practical lithium-sulfur batteries, J. Energy Chem. 76 (2023) 127–145, https://doi.org/10.1016/j.jechem.2022.08.027.

[50] J. He, A. Bhargav, A. Manthiram, High-Performance Anode-Free Li–S Batteries with an Integrated Li 2 S–Electrocatalyst Cathode, ACS Energy Lett. 7 (2022) 583–590, https://doi.org/10.1021/acsenergylett.1c02569.